Published in "Chemical Physics Letters 588: 260–266, 2013"
which should be cited to refer to this work.

Calculation of the $4f^1 \rightarrow 4f^05d^1$ transitions in Ce^{3+}-doped systems by Ligand Field Density Functional Theory

Harry Ramanantoanina [a], Werner Urland [a,b,*], Amador García-Fuente [a], Fanica Cimpoesu [c,*], Claude Daul [a,*]

[a] Department of Chemistry of the University of Fribourg, Chemin du Musée 9, 1700 Fribourg, Switzerland
[b] Institut für Anorganische Chemie der Universität Hannover, Callinstr. 9, D-30167 Hannover, Germany
[c] Institute of Physical Chemistry, Spaiul Independentei 202, Bucharest 060021, Romania

We present a recipe for the calculation of the optical properties of Ce^{3+}-doped systems. The model implies the use of ligand field phenomenology in conjunction with Density Functional Theory (DFT). The particular procedures enable the reliable prediction of the $4f^1 \rightarrow 4f^05d^1$ transitions in $Cs_2NaYCl_6:Ce^{3+}$. The analysis of the doping of Ce^{3+} into the host is accomplished by band structure calculations. The calculated multiplet energy levels are in agreement with the experimental observation, the outlined treatment being, to the best of our knowledge, unprecedented clear and conclusive application of DFT for the rather complex problems of structure and spectroscopy of cerium-doped systems.

1. Introduction

Among the various magnetic and optical properties of systems containing lanthanide ions, determined by the complex electronic structure effects, a special situation is represented by the mechanisms leading to the functioning of rare earth ions in light emitting diodes (LED) technologies. The key effect consists here in the strong f → d dipole allowed transitions. Artificial white light is yet mainly obtained by the combination of a gallium nitride blue LED with an inorganic yellow phosphor, which is yttrium aluminum garnet, $Y_3Al_5O_{12}$, doped with Ce^{3+} [1]. However, the spectrum of known systems do not match well the solar alike day light, the obtaining of the so-called warm-white light being an open quest. Aside of the technological goals, this aim is challenging also for academic approach, since a proper understanding of causal factors can help in the rational tuning of the desired phosphorescence spectrum.

The Ce^{3+} ion is of great interest in computational chemistry since there is only a single valence electron, which makes the theoretical aspects relatively simple, giving further advances into the possibility to predict the optical properties corroborated with the synthesis of the candidate systems or even, prospectively, in advance of the experiment. The analysis of the $4f^1 \rightarrow 4f^05d^1$ transitions in Ce^{3+} complexes is usually approached by phenomenological fit to experimental spectra [2–4] being known also *ab initio* approaches [4–7]. Lesser effort has been done in dealing with Density Functional Theory (DFT), even though methodologies exist, for instance using the early concept of Delta-SCF of Slater [8] or the modern Time Dependent TDDFT routines [9]. A more intuitive way to handle the problem is the application of ligand field theory along the DFT calculation, following the approach of Ligand Field Density Functional Theory (LFDFT), [10] as we have developed first for a single open-shell d- [11] or f-electrons [12] and recently for two open-shell f- and d-electrons [13].

Herein we present a LFDFT approach for the calculation of the optical properties of Ce^{3+} complexes involving two-open-shell f and d. The Hamiltonian which describes such a system is represented in terms of one-electron ligand field and spin–orbit coupling parameters:

$$\mathbf{H} = \mathbf{H_0} + \mathbf{H_{LF}} + \mathbf{H_{SO}}, \quad (1)$$

where the first term $\mathbf{H_0}$ describes the atomic-like body preserving the spherical symmetry, the following components representing the one-electron ligand field ($\mathbf{H_{LF}}$) and the spin–orbit ($\mathbf{H_{SO}}$) interactions. Working in the convention of the Wybourne-normalized crystal field Hamiltonian [14], expanded in the basis of spherical harmonics functions $Y_{k,q}$, both the zero-order and the ligand field terms can be equated with the B_q^k parameters. In the usual single open-shell ligand field problems dedicated either to d- or f-electrons, the $k = 0$ components are ignored but, in the actual two-open-shell problem the relative position of d and f orbitals must be correspondingly defined.

* Corresponding authors. Address: Department of Chemistry of the University of Fribourg, Chemin du Musée 9, 1700 Fribourg, Switzerland. Fax: +41 26 300 9738 (W. Urland, C. Daul).
E-mail addresses: wurland@arcor.de (W. Urland), cfanica@yahoo.com (F. Cimpoesu), claude.daul@unifr.ch (C. Daul).

The Hamiltonian (Eq. (1)) and its components are worked in a spin–orbital basis set, having the series of 24 one-particle states, i.e. 14 spin–orbitals for the $4f^1$ and 10 spin–orbitals for the $4f^05d^1$ electron configuration. Thus, the 24×24 $\mathbf{H_0}$ matrix is presented as following:

$$\mathbf{H}_0 = \begin{pmatrix} B_0^0(f)\mathbf{I_f} & 0 \\ 0 & B_0^0(d)\mathbf{I_d} \end{pmatrix} \quad (2)$$

where $\mathbf{I_f}$ and $\mathbf{I_d}$ are 14 x 14 and 10 x 10 identity matrices, respectively. In fact, only the energy gap $\Delta(fd)$ of the $k = 0$ parameters is required,

$$\Delta(fd) = B_0^0(d) - B_0^0(f) \quad (3)$$

In spite of being labeled with zero subscript, in line with the $k = 0$ elements in the Wybourne formalism, the $\mathbf{H_0}$ includes the effect of ligand field, as spherical average. In the absence of ligand field for the free ion, we shall refer to a $\Delta_0(fd) = h_d - h_f$ energy gap, where h_f and h_d are the energies of the ^2F and ^2D terms originating from the $4f^1$ and $5d^1$ electron configurations of the free Ce^{3+} ion, respectively. From the barycenter of observed spectral terms of the free Ce^{3+} ion, one obtains $\Delta_0(fd) = 49\,943\ cm^{-1}$ [15].

The $\mathbf{H_{LF}}$ Hamiltonian corresponding to the ligand field potential takes full account for the lowering of the symmetry due to the chemical environment of the Ce^{3+} ion center:

$$\mathbf{H}_{LF} = \begin{pmatrix} \mathbf{H}_{LF}(\mathbf{f}) & \mathbf{H}_{LF}(\mathbf{fd}) \\ \mathbf{H}_{LF}(\mathbf{fd})^{T*} & \mathbf{H}_{LF}(\mathbf{d}) \end{pmatrix} \quad (4)$$

where $\mathbf{H_{LF}(f)}$, $\mathbf{H_{LF}(d)}$ and $\mathbf{H_{LF}(fd)}$ are 14×14, 10×10 and 14×10 block matrices, which represent the splitting of the 4f and 5d spin–orbitals. These blocks are made, each, of by two identical subblocks with the respective 7×7, 5×5 and 7×5 dimensions, corresponding to the α and β spin–orbital sets. We worked with double sized matrices in order to introduce the spin–orbit coupling that has matrix elements between the α and β spin–orbitals. In the Wybourne parameterization the ligand field matrices $\mathbf{H_{LF}(f)}$ and $\mathbf{H_{LF}(d)}$ are traceless blocks. A gain of chemical intuition is reached translating the Wybourne-normalized crystal field parameters into the Angular Overlap Model (AOM) [16,17] scheme. The AOM assigns the parameters in accordance to the chemical bonding, e_σ and e_π, having also different sets for the ligand field influence of the f- and d-orbital.

The $\mathbf{H_{SO}}$ Hamiltonian corresponding to the spin–orbit coupling is included because of the large spin–orbit coupling constants encountered in the Ce^{3+} ion embedded in the Cs_2NaYCl_6 crystal host, i.e. $\zeta_{4f} = 624.1$ and $\zeta_{5d} = 792.7\ cm^{-1}$ which were observed experimentally [4]. In this Letter we report a model calculation of the optical properties of the Ce^{3+} ion in a chemical environment, providing a simple recipe based on the LFDFT procedure. The methodology, which takes full account of all interactions in the Hamiltonian given in eq. 1 involves the calculation of the $\Delta(fd)$ (Eq. (3)) and the AOM or B_q^k parameters in a non-empirical way. The model calculation is then applied to the determination of the optical properties of Cs_2NaYCl_6:Ce^{3+}, an example of system which has been widely analyzed either theoretically [4,6] or experimentally [4].

2. Methodology and computational details

The LFDFT calculation presented here involves three steps: (i) an Average of Configuration (AOC), with equal occupation of the 4f-orbital and 5d-orbital is carried out, i.e. $4f^{1/2}5d^{1/2}$ electron configuration. (ii) While these orbitals are kept frozen, the energies of all single determinants within the whole ligand field manifold are calculated, i.e. for the 14 spin–orbital states of the $4f^1$ and for the 10 spin–orbital states of the $4f^05d^1$ electron configurations. These energies are then used to determine the $\Delta(fd)$ parameter and the ligand field potential needed in the present model by a least squares fit. We must point out that the energies of the spin–orbital states obtained running the position of the electron in the frozen Kohn–Sham orbitals previously prepared by the AOC calculation (step i) are subtly different from the orbital energies. (iii) The multiplet splitting of the $4f^1$ and the $4f^05d^1$ electron configurations of the Ce^{3+} ion are then calculated by diagonalizing the Hamiltonian $\mathbf{H}$ given in Eq. (1), having the series of 24 one-particle states as basis.

The molecular DFT calculations reported in this Letter have been carried out by means of the Amsterdam Density Functional (ADF2010) program package [18]. The ADF has the important technical feature of specific input keywords allowing to control orbital and spin populations and generate fractional populations and different Slater Determinants. This leverage is important for the non-routine computational approach demanded by the LFDFT treatment. The local density approximation (LDA) characterized by the Vosko-Wilk-Nussair parameterization [19] of the electron gas data has been used for preliminaries related with geometry consideration. Then the conventional hybrid B3LYP functional [20], i.e. with 20% Hartree–Fock exchange correction has been used for the exchange–correlation energy and potential for the determination of the optical properties of the Ce^{3+} ion. The molecular orbitals were expanded using an uncontracted triple-ζ Slater Type Orbitals (STO) basis set plus two polarization function (TZ2P+) for the Ce atom and an uncontracted triple-ζ STO basis set plus one polarization function (TZP) for the Cl and Na atoms. The LFDFT software running in the Matlab/Octave environment has been developed in Fribourg during the last two decades and is freely available from the authors upon request.

We have also carried out electronic and structural calculations of the periodic system Cs_2NaYCl_6 with the Vienna *Ab initio* Simulation Package (VASP) [21] and the Projector Augmented Wave method (PAW) [22]. This calculation allows to analyze the distortion induced in the lattice structure by the substitutional doping of the Ce^{3+} ion taking into account the periodicity of the infinite system, which is not possible with the molecular calculation. For the exchange–correlation potential we used the LDA [19], as well as the Generalized Gradient Approximation (GGA) parameterization by Perdew et al. [23]. The band structure calculations were done using a plane-wave basis set with a cutoff energy of 350 eV. The geometry optimization of cell parameters and site coordinates was performed until forces were smaller than 0.001 eV/Å. We simulated a periodic cubic structure of 40 atoms and a lattice constant of 10.740 Å, in which we introduce a Ce^{3+} impurity into an Y^{3+}-site. This means that we have an impurity concentration of 25% (a Ce^{3+} ion in each fourth Y^{3+}-site) and a distance between nearest impurities of 10.740 Å. We found this unit cell size to be large enough so that the interactions between impurities are negligible, as test made with larger unit cells gave similar results.

3. Results and discussion

A recent work published by the authors [13] describes the analysis of the general $4f^n \rightarrow 4f^{n-1}5d^1$ transitions in lanthanide complexes. The general methodology named LFDFT was applied for the characterization of the optical properties of Pr^{3+} doped into Cs_2KYF_6 crystallizing in the elpasolite structure type, in order to emphasize the microscopic origin of the so-called quantum-cutting process. It has been shown that the DFT calculation based on the hybrid B3LYP functional gives a reasonable agreement with the experimental observation [13]. The energy gap between the 4f and 5d configurations of the Ce^{3+} ion is represented by the $\Delta(fd)$

parameter, which also describes the influence of a spherical environment as given in Eq. (3). In the absence of ligand field interaction, we calculated the $\Delta_0(fd)$ parameter using LFDFT method, where a value of 49943 cm^{-1} is deduced experimentally. [15] The calculated together with the experimental multiplet energy splitting of the free Ce^{3+} ion are presented in Figure 1, while the hybrid functional was used along the LFDFT procedure.

Taking into account the spin–orbit coupling, the ground state ^2F of the Ce^{3+} ion splits in two components: the $^2F_{7/2}$ and $^2F_{5/2}$ terms. In the same way, the excited state ^2D splits into $^2D_{5/2}$ and $^2D_{3/2}$ terms. The calculated energy levels corresponding to these four spin–orbit terms are calculated and presented in Figure 1, in which the spin–orbit coupling constants have been calculated using the approach of ZORA relativistic [24] available in the ADF program package [24] where $\zeta_{4f} = 738.5$ and $\zeta_{5d} = 990.4\ cm^{-1}$ were found at the B3LYP level of theory. These calculated spin–orbit coupling constants for the free Ce^{3+} ion are in good agreement with the experimental data [15] Although B3LYP functional was found suitable to represent the optical properties of the Pr^{3+} ion [13], it is seen from Figure 1 that the conventional B3LYP parameterization, i.e. with 20% Hartree–Fock exchange correction fails to represent the splitting pattern, in other words the $\Delta_0(fd)$ parameter is overestimated by the pure exchange–correlation part. Moreover, the greater is the amount of the Hartree–Fock exchange correction included in the hybrid parameterization, the more accurate are the results as the $\Delta_0(fd)$ parameter decreases (Figure 1). This happens until a Hartree–Fock exchange correction of 80% (Figure 1). At higher percentage, the $\Delta_0(fd)$ parameter starts to be underestimated, suggesting however the absolute necessity of DFT content in the exchange–correlation energy and potential.

The Ce^{3+} ion is doped into the Cs_2NaYCl_6 host, replacing the trivalent Y^{3+} ion, as it is observed experimentally [4]. Therefore the Ce^{3+} ion is coordinated with six chloride ligands forming an octahedral arrangement. We have carried out a structural optimization within the plane-wave band structure calculation of the infinite periodic system. The results show that the substitution doping of an Y^{3+}-site with Ce^{3+} ion mainly affects the positions of its first neighbors, namely the six chloride ligands whereas the displacement of the remaining atoms is negligible. In Figure 2 we show the dependence of the potential energy with the distance between the Ce^{3+} ion and the chloride ligands. We found an equilibrium distance of 2.702 Å with LDA calculation and of 2.714 Å with GGA, in good agreement with the further molecular calculation (see Table 1) and the experimental data. However, the plane-wave band structure calculation does not allow to control molecular orbitals and their occupation schemes in the manner demanded by the LFDFT approach, so that a cluster containing the cerium site, selected as a cut from the lattice, has to be used in subsequent molecular calculations, in order to generate the different excited states. The selected cluster contains a central Ce^{3+} ion, the nearest neighbors (i.e. six chloride ligands) and the next nearest neighbors (i.e. six Na^+ ions). This cluster calculation is expected to reproduce reasonably the situation of the Ce^{3+} ion embedded in the crystal in a Y^{3+}-site. A geometry optimization procedure is carried out in the molecular system in order to determine the bond length between the Ce^{3+} ion and the chloride ligands following a totally symmetric displacement of the chloride cage, in the case of different molecular orbital configuration.

In the octahedral environment, the 4f-orbital of the Ce^{3+} ion splits into a_{2u}, t_{2u} and t_{1u} representative of the irreducible representations (irreps) of the O_h point group, while the 5d-orbital splits into t_{2g} and e_g. In Table 1 we present the calculated geometry of the cluster as function of different occupation schemes, nevertheless making the assumption that the spin–orbit interaction does not affect too much the optimized geometry.

A bond length of 2.619 Å between the Y^{3+} ion and the chloride ligands was found experimentally in Cs_2NaYCl_6 crystallizing in the elpasolite structure type [25]. While doped with Ce^{3+}, the size of the Y^{3+}-site always increases (cf. Table 1 and Figure 2) in accordance to the estimation by Shannon radii [26] of Ce^{3+} and Cl^- ions

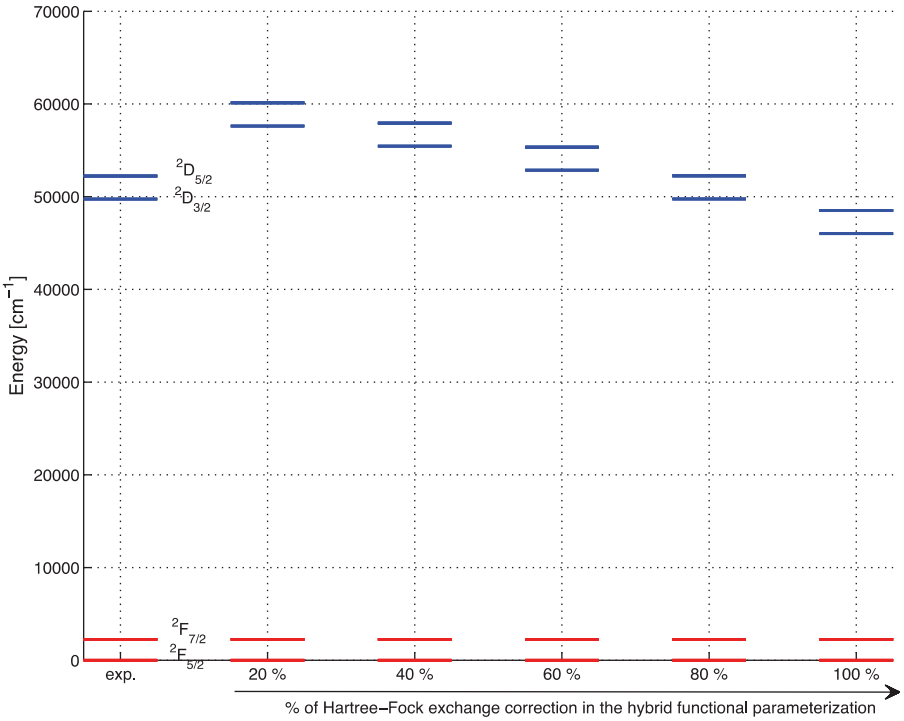

Figure 1. Experimental (exp.) and calculated LFDFT multiplet energy levels at the hybrid level of theory while the percentage of the Hartree–Fock exchange correction included in the hybrid parameterization is varied; corresponding to the $4f^1$ (in red) and $4f^05d^1$ (in blue) electron configurations of the Ce^{3+} ion. (For interpretation of the references to color in this figure legend, the reader is referred to the web version of this article.)

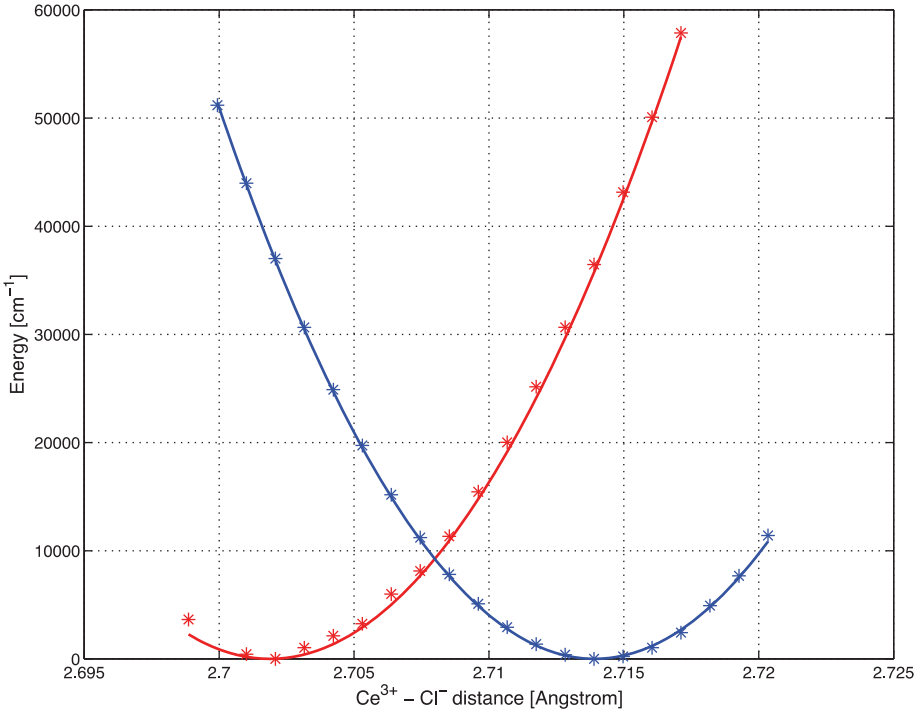

Figure 2. Total energy, referred to the minimal energies, of the infinite periodic system Cs_2NaYCl_6 with a Ce^{3+} impurity in an Y^{3+}-site, as a function of the distance between the Ce^{3+} impurity and its six nearest neighbors, which are chloride ligands; corresponding to the LDA (in red) and GGA (in blue) calculations. (For interpretation of the references to color in this figure legend, the reader is referred to the web version of this article.)

Table 1
Calculated DFT bond length d (in Å) between Ce^{3+} and Cl^{-} ions by doping of the octahedral Y^{3+}-site in Cs_2NaYCl_6 in terms of different molecular orbital (MO) occupation schemes.

Origin of state	MO Occupation	Electronic state	d
$4f^{\frac{1}{7}}5d^{\frac{1}{2}}$	$a_{2u}^{\frac{1}{14}}\, t_{2u}^{\frac{3}{14}}\, t_{1u}^{\frac{3}{14}}\, t_{2g}^{\frac{3}{10}}\, e_g^{\frac{2}{10}}$	–	2.6955
$4f^{1}5d^{0}$	$a_{2u}^{2}\, t_{2u}^{6}\, t_{1u}^{6}\, t_{2g}^{0}\, e_g^{0}$	–	2.7256
	$a_{2u}^{1}\, t_{2u}^{6}\, t_{1u}^{6}\, t_{2g}^{0}\, e_g^{0}$	$^2A_{2u}$	2.7240
	$a_{2u}^{0}\, t_{2u}^{1}\, t_{1u}^{6}\, t_{2g}^{0}\, e_g^{0}$	$^2T_{2u}$	2.7261
	$a_{2u}^{0}\, t_{2u}^{6}\, t_{1u}^{1}\, t_{2g}^{0}\, e_g^{0}$	$^2T_{1u}$	2.7257
$4f^{0}5d^{1}$	$a_{2u}^{0}\, t_{2u}^{6}\, t_{1u}^{6}\, t_{2g}^{\frac{3}{5}}\, e_g^{\frac{2}{5}}$	–	2.6698
	$a_{2u}^{0}\, t_{2u}^{6}\, t_{1u}^{6}\, t_{2g}^{1}\, e_g^{0}$	$^2T_{2g}$	2.6624
	$a_{2u}^{0}\, t_{2u}^{6}\, t_{1u}^{6}\, t_{2g}^{0}\, e_g^{1}$	^2E_g	2.6880

for such an octahedral coordination. The calculated bond lengths for the electronic states originating from the $4f^1$ electron configuration of the Ce^{3+} ion are almost equal, whereas a difference is found for the two states $^2T_{2g}$ and ^2E_g originating from the $4f^05d^1$ electron configuration. This is in line with the small implication of the f electrons in the bonding, while coordination effect of lanthanide ions is merely ensured by the empty 5d virtuals, in the ground state [27]. This is also correlated with the apparently intriguing fact that the system in the $4f^05d^1$ excited configuration shows sensibly shorter coordination bonds as compared to those in the $4f^1$ ground configuration.

Moreover, except for the case of the $^2A_{2u}$ state, the other electronic states tabulated in Table 1 (i.e. $^2T_{1u}$, $^2T_{2u}$, $^2T_{2g}$ and ^2E_g) are degenerate states. Meanwhile these states undergo an Jahn–Teller distortion [28], like in the case of the well-known vibronic coupling between the $^2T_{2g}$ electronic state with e_g and t_{2g} vibrational modes in cubic symmetry ($T_{2g} \otimes (e_g + t_{2g})$). Accordingly, various geometries belonging to the D_{4h} and D_{3d} epikernel subgroups of the O_h point group appear with relatively small Jahn–Teller stabilization energies. However, these energies are mostly smaller than those determined by spin–orbit coupling, which for instance already splits the $^2T_{2g}$ state into two states labeled Γ_{7g} and Γ_{8g} in the $O*$ double group, allowing us to neglect the Jahn–Teller effect.

In Table 1 (line 3 and line 7) two geometries are presented and determined by means of the AOC approach. The AOC occupation of the Kohn–Sham orbital is a restricted self consistent field computation to represent the partially filled shell originating from the 4f- and 5d-orbital of the Ce^{3+} ion. The electron is evenly distributed upon first the 14 spin–orbitals of 4f-orbital, then the 10 spin–orbitals of the 5d-orbital of the Ce^{3+} ion. In this way, the densities have the symmetry of the external potential, i.e. belong to the totally symmetric representation of the point group under which the Hamiltonian is invariant. This AOC type geometry optimization often has been used in LFDFT [10–13] and allows to obtain the vertical transition energies of the complex being analyzed upon the specific electron configuration defined in the AOC scheme. Hence, the vertical absorption energies and the vertical emission energies of the Ce^{3+} ion doped into the Y^{3+}-site are calculated and the corresponding ligand field parameters are extracted and presented in Table 2. These vertical transition energies are obtained first for the absorption considering the bond length between the Ce^{3+} ion and the chloride ligands as 2.726 Å and secondly for the emission considering this bond length as 2.670 Å, according to the geometries presented in Table 1.

Although the multiplet energy splitting of the 4f-orbital of the Ce^{3+} ion is slightly underestimated if compared to the experimental data (see Table 3), the LFDFT parameters presented in Table 2 are in general in good agreement to the experimental fitted parameters. The two sets of parameters related once to absorption and secondly to emission are different, especially for the case of the 5d-orbital. In the emission as the bond lengths between the Ce^{3+} ion and the chloride ligands are shorter, the splitting pattern of the 5d-orbital is much more pronounced than that occurring in

Table 2
Fitted ligand field parameters (in cm^{-1}) deduced from LFDFT (using the hybrid B3LYP functional) and experimental values: $\Delta(fd)$, AOM parameters e_σ and e_π and the Wybourne normalized crystal-field parameters B_q^k in terms of the bond length d (in Å) between the Ce^{3+} ion and the chloride ligands.

	Experimental	Theoretical parameters	
		Absorption	Emission
d	–	2.7256	2.6698
$\Delta(fd)$	36015.4[a]	36512.5	35927.7
e_σ (f)	434.1[b]	405.0	393.3
e_π (f)	169.7[b]	127.5	148.7
e_σ (d)	11059.7[b,c]	11052.4	12894.8
e_π (d)	3686.6[b,c]	3692.9	4306.3
B_0^4 (f)	2208[a]	2013.8	1992.9
B_0^6 (f)	250[a]	297.7	237.2
B_0^4 (d)	38709[a]	38609.7	45064.5

[a] These parameters are taken from Ref. [4].
[b] Deduced AOM parameters from the Wybourne normalized crystal-field parameters in Ref. [4] using the correlation factors given in Ref. [13].
[c] With the ratio $e_\sigma(d)/e_\pi(d) = 3$.

the absorption, whereas for both transitions the splitting pattern of the 4f-orbital looks similar (see Table 3). It is noteworthy to highlight that although the change of the bond length between the Ce^{3+} ion and the chloride ligands does not affect the determined AOM parameters corresponding to the 4f-electrons, the presence of the Na^+ ions in our cluster calculations must interfere with the parameters as stated by Atanasov et al. [29] have determined that the AOM $e_\sigma(f)$ parameter decreases in the presence of point charges, as surrogate for the effect of Na^+ ions considered explicitly in our case. In turn, the $e_\pi(f)$ quantities are particularly unaffected. This is because of the small implication of the unoccupied 3s-orbital of the Na^+ ions into the molecular orbital of the cluster. Given the O_h ligand field symmetry, a symmetry adapted linear combination of the 3s-orbital of the six Na^+ ions forms the basis of a_{1g}, e_g and t_{1u} irreps. This latter one, while combined to the one originating from the splitting of the 4f-orbital of the Ce^{3+} ion, contributes to stabilize the energy of the resulting molecular orbital within the t_{1u} irrep, *ergo*, lowering the value of the AOM parameter $e_\sigma(f)$ independently to that for the $e_\pi(f)$.

The quantities presented in Table 2 are used to parameterize the Hamiltonian **H** shown in Eq. (10). The multiplet energy splittings corresponding to the $4f^1$ and $4f^05d^1$ electron configurations of the Ce^{3+} ion are then obtained by diagonalizing this Hamiltonian. The eigenvalues of the Hamiltonian **H** (eq. 1) are presented in Figure 3 for instance for the calculated absorption transitions, taking into account successively the influence of $\mathbf{H_0}$, $\mathbf{H_{LS}}$ and $\mathbf{H_{SO}}$ as it is defined in Eq. (1).

Considering $\mathbf{H_0}$ (Eq. (2)), two electronic states are obtained: the ground state ^2F and the excited state ^2D, whose degeneracies are 14 and 10, respectively. The octahedral ligand field parameterized in the $\mathbf{H_{LF}}$ Hamiltonian (Eq. (4)) splits these states into the following irreps of the O_h point group: $^2F \rightarrow {}^2A_{2u}+{}^2T_{2u}+{}^2T_{1u}$ and $^2D \rightarrow {}^2T_{2g}+{}^2E_g$. The eigenvalues of the $\mathbf{H_{LF}}$ (Eq. (4)) matrix give the energies of these electronic states. Given the high symmetry, the ligand field energy levels or, equivalently, the spectral term energies of $4f^1$ and $4f^05d^1$ configurations, can be expressed in the following analytical formulas, using the Wybourne parametric scheme:

$$E(^2A_{2u}) = B_0^0(f) - \frac{4}{11}B_0^4(f) + \frac{8}{143}B_0^6(f) \quad (5a)$$

$$E(^2T_{2u}) = B_0^0(f) - \frac{2}{33}B_0^4(f) - \frac{60}{143}B_0^6(f) \quad (5b)$$

$$E(^2T_{1u}) = B_0^0(f) + \frac{2}{11}B_0^4(f) + \frac{100}{429}B_0^6(f) \quad (5c)$$

$$E(^2T_{2g}) = B_0^0(d) - \frac{4}{21}B_0^4(d) \quad (5d)$$

$$E(^2E_g) = B_0^0(d) + \frac{2}{7}B_0^4(d) \quad (5e)$$

The presentation of the energies of the spectral terms in Figure 3 are related with the $B_0^0(f) = 0$ convention and the $B_0^0(d) = \Delta(fd)$ equivalence. Alternatively, one may choose the $B_0^0(f)$ in order to set the energy of the ground state $^2A_{2u}$ in zero in respect to the AOM formulation, where the energy of this electronic ground state is zero by symmetry because the octahedral ligand field does not contains this representation in the perturbation. The conversion of the Wybourne-normalized crystal field parameters into the AOM ones is outlined in a precedent work [13]. In the case of the f-shell, the number of parameters in AOM vs. Wybourne schemes is identical, making their conversion straightforward. However in the d-shell the AOM implies two parameters while the symmetry and Wybourne scheme demand only one. The redundancy of the AOM parameterization is usually reduced imposing the $e_\sigma(d)/e_\pi(d) = 3$ ratio. This ratio is used to compare with experimental data, where in O_h symmetry $10Dq$ is the only relevant parameter, and can be calculated from *ab initio* methodology as seen in Table 2.

The spin–orbit components resulted from the split of the O_h spectral terms, in the Bethe notation of the irreps of the O∗ double group, are $^2A_{2u} \rightarrow \Gamma_{7u}$, $^2T_{2u} \rightarrow \Gamma_{7u} + \Gamma_{8u}$ and $^2T_{1u} \rightarrow \Gamma_{6u} + \Gamma_{8u}$ for the $4f^1$ electron configuration; while $^2T_{2g} \rightarrow \Gamma_{7g} + \Gamma_{8g}$ and $^2E_g \rightarrow \Gamma_{8u}$ for the $4f^05d^1$ case. *In fine* 24 eigenvalues, 12 Kramers doublet are determined out of the diagonalization of the Hamiltonian **H** (Eq. (1)) and presented in Figure 3 in terms of the spectroscopic terms listed above for the absorption transitions of Ce^{3+}-doped Cs_2NaYCl_6. These eigenvalues are also numerically presented in Table 3

Table 3
Experimental versus calculated multiplet energy levels (in cm^{-1}) referred to the lowest energy level at the B3LYP level of theory, corresponding to the absorption and emission transitions of Ce^{3+}-doped into the Cs_2NaYCl_6.

State			Deg. [a]	Exp. [b]	Theoretical	
					Absorption	Emission
^2F	$^2A_{2u}$	Γ_{7u}	2	0	0.0	0.0
	$^2T_{2u}$	Γ_{8u}	4	597	534.6	539.5
		Γ_{7u}	2	2167	2162.0	2162.8
	$^2T_{1u}$	Γ_{8u}	4	2691	2628.7	2632.9
		Γ_{6u}	2	3085	3015.1	2997.4
^2D	$^2T_{2g}$	Γ_{8g}	4	28,196	30355.2	28548.2
		Γ_{7g}	2	29435	31594.3	29780.3
	^2E_g	Γ_{8g}	4	47125	49237.2	50489.9

[a] Deg. stands for the degeneracy of the electronic states.
[b] These energy levels are calculated using the experimental parameter given in Table 2 with the spin–orbit coupling constants $\zeta_{4f} = 624.1$ cm^{-1} and $\zeta_{5d} = 792.7$ cm^{-1} and are also displayed in Refs. [4] and [6].

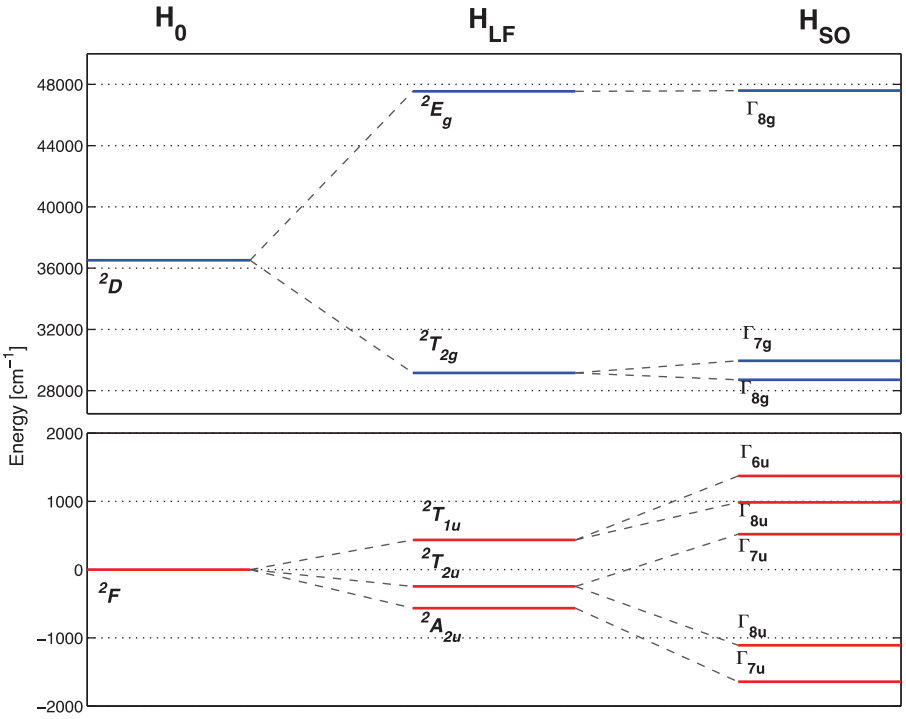

Figure 3. Schematic representation of the calculated multiplet energy levels for the absorption transitions of Ce^{3+}-doped Cs_2NaYCl_6 corresponding to the $4f^1$ (in red) and $4f^05d^1$ electron configurations (in blue) of the Ce^{3+} ion, considering successively the effect of $\mathbf{H_0}$, $\mathbf{H_{LF}}$ and $\mathbf{H_{SO}}$ defined in the Hamiltonian $\mathbf{H}$ (Eq. (1)). The energy of the spectral term ^2F in the presented model is taken as origin of the energy. The spectroscopic terms are highlighted. (For interpretation of the references to color in this figure legend, the reader is referred to the web version of this article.)

for the absorption and emission transitions together with the experimental observation.

Our calculations for the $4f^1 \rightarrow 4f^05d^1$ transitions of Ce^{3+} ion doped into Cs_2NaYCl_6 give the LFDFT methodology predicting more accurately the optical properties of Ce^{3+} ion embedded in a crystal host than other existing treatment. Hu et al. [6] have extracted the crystal field parameters for lanthanide ions from non-empirical calculations. Their work reports the doping of the Ce^{3+} ion into Cs_2NaYCl_6 like the present case using the DV-Xα method. The DV-Xα, which stands for Discrete Variational Xα [30] is an all electron molecular orbital calculation based on the Hartree–Fock–Slater equation using the simple Xα expression for the exchange functional. Although the results Hu et al. [6] have presented are in overall acceptable, the methodology fails to reproduce the $\Delta(fd)$ parameter, as they obtain 13 806 cm^{-1} [6] instead of the experimentally observed energy, i.e. 36 015 cm^{-1}. The problem appears in previous work, for instance the same methodology applied to Ce^{3+} doped into CaF_2 gave a $\Delta(fd)$ parameter of 54 145 cm^{-1}, while the experimental one is 44 929 cm^{-1} [6], or Gracia et al. [31] also reports the calculation of the $4f^1 \rightarrow 4f^05d^1$ transitions of Ce^{3+} ion doped into YAG using the same DV-Xα method, where they obtained a $\Delta(fd)$ parameter of 33 622 cm^{-1} [31] instead of the experimental one of 36 570 cm^{-1}. A long list of similar investigations is collected throughout the paper of Hu et al. [6] where they make a comparative study between their results with earlier published paper. The same trend is noticed, since the $\Delta(fd)$ parameter always mismatches the experimental deduced value, finally forcing them to use the experimentally fitted $\Delta(fd)$ parameter to calculate the multiplet energy levels similar to those we presented in Table 3. The *ab initio* wave function theory based calculations of Tanner et al. [4], also accounts for the optical properties of Ce^{3+} ion doped into Cs_2NaYCl_6. Aside measuring high quality emission/absorption spectra of Ce^{3+} doped into Cs_2NaYCl_6, Tanner et al. [4] have calculated the corresponding optical properties in order to validate their experimental observation. Their calculated multiplet energy levels give a mean average deviation of 260 cm^{-1}, which, in our opinion, is not relatively significant while compared to the results we present in Table 3. The deviations in the cited works results mainly from the calculated energy of the Γ_{8u} state originating from the $^2T_{2u}$ state, 831 cm^{-1} [4] instead of the 597 cm^{-1} experimentally observed energy. Our LFDFT calculation slightly deviates from the experimental observation especially for the energy level calculated for the ^2E_g (Γ_{8g}) state in the emission transition (Table 3), which is probably due to the slight difference between the geometries obtained for the $^2T_{2g}$ and ^2E_g terms (Table 2). The computational details might be extended in order to diminish this deviation, considering that we ignored by computational setting (equal smearing of electron population inside degenerate orbitals) the implication of possible Jahn–Teller distortions. Having similar performances with the Tanner et al. [4] approach, our DFT based approach is however simpler and more transparent as compared to the rather complicated theorization and a time-consuming calculations presented in the mentioned works. This is a non-trivial methodological advance, applicable to other systems of interest. At the same time the presented numerical results and the extracted ligand field parameters are useful in the interpretation of the spectral properties of Ce^{3+}-doped compounds and the prospection in applications related with the optical manifestations.

4. Conclusion

The reliable prediction of the $4f^n \rightarrow 4f^{n-1}5d^1$ transitions in lanthanide ion-doped compounds offers a significant progress in LED technologies. The calculation of the optical properties, before the time-and-resource consuming synthesis of the corresponding lanthanide compounds, is a desideratum helping in the prospective prediction of warm-white light generator materials. The LFDFT approach applied in this Letter to the system Cs_2NaYCl_6:Ce^{3+} represents, due to its relation to ligand field theory, a transparent way

amongst the different available models to predict the optical transition energies.

In this work, the optical transition energies are calculated by the treatment of the Ce^{3+} ion center in a perturbation approach, involving one-electron interactions due to ligand field influence and spin–orbit coupling effect. The representation of the Hamiltonian in terms of these interactions makes the general methodology independent to symmetry constrain giving further insight into the calculation of the Ce^{3+} ion even in a C_1 ligand field instead of the octahedral example given in this Letter. The LFDFT procedure requires three steps where the most fundamental one, in which the method itself takes its origin, is the representation of the open shell 4f- and 5d-electrons density in a totally symmetric reference. This totally symmetric density is obtained in the AOC occupation scheme of the molecular orbitals, whose the main characters possess the 4f- and 5d-orbital of the Ce^{3+} ion. This methodology has shown once again to be a reliable DFT tool for the non-empirical determination of the optical properties of lanthanide ion-doped compounds.

Acknowledgments

This work is supported by the Swiss National Science Foundation. Support from the UEFISC-CDI research grant PCCE 9/2010 is also acknowledged.

References

[1] S. Nakamura, G. Fasol, The Blue Laser Diode, Springer, Berlin, 1997.
[2] R.W. Schwartz, P.N. Schatz, Phys. Rev. B 8 (1973) 3229.
[3] R.W. Schwartz, N.J. Hill, J. Chem. Soc. Faraday II (1974) 124.
[4] P.A. Tanner, C.S.K. Mak, N.M. Edelstein, K.M. Murdoch, G. Liu, J. Huang, L. Seijo, Z. Barandiaran, J. Am. Chem. Soc. 125 (2003) 13225.
[5] Z. Barandiaran, L. Seijo, J. Chem. Phys. 89 (1988) 5739.
[6] L. Hu, M.F. Reid, C.-K. Duan, S. Xia, M. Yin, J. Phys. Condens. Matter 23 (2011) 045501.
[7] J. Wen, L. Ning, J. Phys. Chem. C 38 (2012) 20513.
[8] J.C. Slater, Adv. Quantum Chem. 6 (1972) 1.
[9] M.E. Casida, J. Mol. Struct. Theochem. 914 (2009) 3.
[10] M. Atanasov, C. Daul, Chimia 59 (2005) 504.
[11] M. Atanasov, C. Daul, C. Rauzy, Struct. Bond. 106 (2004) 97.
[12] A. Borel, L. Helm, C. Daul, Chem. Phys. Lett. 383 (2004) 584.
[13] H. Ramanantoanina, W. Urland, F. Cimpoesu, C. Daul, Phys. Chem. Chem. Phys. 15 (2013) 13902.
[14] S. Hüfner, Optical Spectra of Transparent Rare Earth compounds, Academic Press, New York, 1978.
[15] A. Kramida, Y. Ralchenko, J. Reader, NIST Atomic Spectra Database (ver. 5.0), [Online]. Available: http://physics.nist.gov/asd [2013, June 21], National Institute of Standards and Technology, Gauthersburg, MD, 2013.
[16] C. Schäffer, C. Jørgensen, Mol. Phys. 9 (1965) 401.
[17] W. Urland, Chem. Phys. 14 (1976) 393.
[18] G. te Velde, F.M. Bickelhaupt, E.J. Baerends, C. Fonseca Guerra, S.J.A. van Gisbergen, J.G. Snijders, T. Zigler, J. Comp. Chem. 22 (2001) 931.
[19] S. Vosko, L. Wilk, M. Nussair, Can. J. Phys. 58 (1980) 1200.
[20] P.J. Stephens, F.J. Devlin, C.F. Chabalowski, M.J. Frisch, J. Phys. Chem. 98 (1994) 11623.
[21] G. Kreese, J. Furtmüller, Comput. Mater. Sci. 6 (1996) 15.
[22] P.E. Blöchl, Phys. Rev. B 50 (1994) 17953.
[23] P. Perdew, K. Burke, M. Ernzerhof, Phys. Rev. Lett. 77 (1996) 3865.
[24] E. van Lenthe, E.J. Baerends, J.G. Snijders, J. Chem. Phys. 99 (1993) 4597.
[25] C. Reber, H.U. Guedel, G. Meyer, T. Schleid, C.A. Daul, Inorg. Chem. 28 (1989) 3249.
[26] R.D. Shannon, Acta Crys. A 32 (1976) 751.
[27] M. Ferbinteanu, A. Zaharia, M.A. Girtu, F. Cimpoesu, Cent. Eur. J. Chem. 8 (2010) 519.
[28] H.A. Jahn, E. Teller, Proc. R. Soc. A 161 (1937) 220.
[29] M. Atanasov, C. Daul, H.U. Güdel, T.A. Wesolowski, M. Zbiri, Inorg. Chem. 44 (2005) 2954.
[30] A. Rosen, D.E. Ellis, J. Chem. Phys. 62 (1975) 3039.
[31] J. Gracia, L. Seijo, Z. Barandiaran, D. Curulla, H. Niemansverdriet, W. van Bennip, J. Lumin. 128 (2008) 1248.